Food Biophysics (2009) 4:199–212
DOI 10.1007/s11483-009-9118-7

ORIGINAL ARTICLE

The Effect of Tripalmitin Crystallization on the Thermomechanical Properties of Candelilla Wax Organogels

Jorge F. Toro-Vazquez · Maritza Alonzo-Macias · Elena Dibildox-Alvarado · Miriam A. Charó-Alonso

Received: 14 March 2009 / Accepted: 3 June 2009 / Published online: 17 June 2009

Abstract The effect of tripalmitin (TP) crystallization on the thermomechanical properties of organogels developed with candelilla wax (CW) was investigated using safflower oil high in triolein (HOSFO) as the liquid phase. Factorial combinations of CW (i.e., 0–3%) and TP (i.e., 0–1%) in the HOSFO were used to develop organogels at three different temperatures (T_{set}). The onset of crystallization (T_g) during the cooling stage (10 °C/min), the melting temperature (T_M), and the corresponding heat of melting (ΔH_M) of the organogels were determined by differential scanning calorimetry. Results showed that, without CW, the crystallization of TP in the HOSFO at the concentrations and T_{set} investigated (i.e., −10 °C to 25 °C) did not develop a three-dimensional network that provided significant viscoelasticity (i.e., solid-like behavior) to the HOSFO. The CW developed organogels in the HOSFO with T_M's that increased from ≈30.5 °C up to ≈42.5 °C as a function of CW concentration. In contrast, in the CW–1% TP system, the co-crystallization of TP and CW resulted in organogels with T_M's that varied just between 36 °C and 38 °C, independent of the CW concentration. Higher elastic modulus (G′) and yield stress (σ^*) were obtained with 3% CW–1.0% TP organogels than with organogels developed just by CW, particularly at T_{set}'s of −5 °C and 15 °C. This research showed that co-crystallization of TP and CW, occurring at different extent as a function of T_{set}, resulted in organogels with thermomechanical properties different from the ones showed by CW organogels. The results showed that co-crystallization of triacylglycerides with CW might be a useful alternative to tailor particular physicochemical properties associated to a specific functionality (i.e., melting profile and texture). Organogelation of vegetable oil might be used to develop *trans*-free vegetable-oil-based spreads and coatings and also novel food products with new textural perceptions for the consumers.

Keywords Tripalmitin crystallization · Candelilla wax · Organogelation · *Trans*-free

J. F. Toro-Vazquez (✉) · E. Dibildox-Alvarado · M. A. Charó-Alonso
Facultad de Ciencias Quimicas–CIEP,
Universidad Autónoma de San Luis Potosi,
Av. Dr. Manuel Nava 6, Zona Universitaria,
San Luis Potosí, San Luis Potosí 78210, Mexico
e-mail: toro@uaslp.mx

M. Alonzo-Macias
DIPA-PROPAC, Universidad Autónoma de Queretaro,
Santiago de Querétaro, Mexico

Introduction

Candelilla wax (CW) is a worldwide recognized food additive approved by the FDA (under regulations 21CFR, 175.105, 175.320, 176.180). Our previous investigation with CW have shown that, under several time-temperature conditions, the *n*-alkanes present in CW (i.e., hentriacontane, $C_{31}H_{64}$) develop thermoreversible organogels in safflower oil.[1,2] In general, the results showed that the use of low gel setting temperatures (i.e., 5 °C vs. 25 °C) and low cooling rates (i.e., 1 °C/min vs. 10 °C/min) provided gels with higher viscoelastic properties.[2] In particular, the organogels developed with 3% CW showed textural properties of potential interest to the food industry.[1] Organogelation using vegetable oils as the liquid phase is a promising alternative to modify the physical properties of vegetable oils without the use of chemical process that results in the formation of *trans*-fatty acids. This opens new alternatives to produce *trans*-free vegetable-oil-based spreads and coatings and novel food products with new textural perceptions for the consumers.

Vegetable oils contain different types of triacylglycerides (TAGS), some of them able to crystallize under similar time–temperature conditions to that of CW components (i.e., hentriacontane). Recently, Martini et al.[3] showed that the addition of sunflower oil waxes modified the crystallization of anhydrous milk fat crystallization. These authors suggested that waxes might be used as additives to modify TAGS crystal networks and, therefore, their textural properties. However, Martini et al.[3] did not do any rheological or textural measurement. The development of such crystallized mixed system ought to have implications in the microstructural organization of the organogel and, therefore, in its thermomechanical properties. Within this framework, the objective of this paper is to establish the effect of tripalmitin (TP) crystallization on the thermomechanical properties of CW organogels developed using safflower oil high in triolein (HOSFO) as the liquid phase. The experiment design used was based on the use of CW–TP mixtures dissolved in HOSFO and processed under time–temperature conditions where the concomitant crystallization of TP and CW occurred.

Materials and Methods

Vegetable oil, Candelilla Wax, and Tripamitin Analysis

HOSFO was obtained from a local producer (Coral Internacional, San Luis Potosí, Mexico). Micronized high-purity CW was supplied from Multiceras (Monterrey, Mexico), and the ≈85% TP was obtained from Sigma Chemical (Saint Louis, MO, USA). The HOSFO and the CW were analyzed by high-performance liquid chromatography and capillar gas chromatography (GC)-mass spectrometry as described previously.[1] Fatty acids profile of TP was analyzed by GC. The composition is reported as the mean±standard deviation of at least two independent determinations (n=2).

Dynamic Gelation/Crystallization of CW and TP Solutions in HOSFO

For preliminary studies, CW (0.5–6% wt/vol) or TP (0.5–5% wt/vol) was dissolved in HOSFO by heating (90 °C) under constant agitation (30 min). Samples of these solutions (10 mL) were stored in test tubes at 5 °C and 25 °C for visual evaluation after 24 h of storage. The dynamic crystallization and melting thermograms of these solutions were obtained by differential scanning calorimetry (DSC) using a TA Instruments Model Q1000 (TA Instruments, New Castle, DE, USA). After calibration of the equipment as previously described,[4] samples (≈5–7 mg) were sealed in aluminum pans, heated at 90 °C for 30 min, and then cooled to −80 °C at a rate of 10 °C/min. After 2 min at −80 °C, the system was heated up to 90 °C (5 °C/min). Based on the thermograms and the visual appearance of the systems developed after 24 h of storage at 5 °C and 25 °C, different concentrations of CW (i.e., 0%, 0.5%, 0.75%, 1%, and 3%) and TP (i.e., 0%, 0.5%, and 1%) were selected for further investigation. In general, the CW concentrations selected had an onset of gelation below 40 °C with a melting peak below 45 °C. In addition, after 24 h at 5 °C, all the CW concentrations selected developed gels that remained at the bottom of the test tubes after turning the tubes upside down. In contrast, although the 0.5% and 1% TP concentrations investigated crystallized in the HOSFO after 24 h of storage at 5 °C and 25 °C, these systems did not develop a three-dimensional network that resulted into a gel-like structure.

Experimental Design to Investigate Organogel Formation in CW–TP Solutions

The CW–TP solutions investigated by DSC resulted from the factorial combinations of the selected CW (0%, 0.5%, 0.75%, 1%, and 3%) and TP (0%, 0.5%, and 1%) concentrations. The CW–TP solutions with 0% CW (and 0.5% or 1% TP) or 0% TP (and 0.5%, 0.75%, 1%, or 3% CW) were used as control systems, and their thermograms were used to identify the thermal transitions corresponding to CW or TP in the CW–TP systems. The isothermal temperatures (T_{set}) investigated were established based on the thermograms of the CW–TP solutions in the HOSFO so that crystallization/gelation of TP and CW occurred at different degrees of supercooling (see later in "Results and Discussion"). Thus, after heating (90 °C for 30 min) samples (≈5–7 mg) of the CW–TP solutions sealed in aluminum pans, the systems were cooled down at a rate of 10 °C/min (i.e., non-isothermal stage) until achieving a particular T_{set}. After 60 min at this T_{set} (i.e., isothermal stage), the melting thermogram was obtained by heating at 5 °C/min until attaining 90 °C. With the equipment software (TA-Instruments Universal Analysis 2000, v. 4.0), the beginning of the exotherm for CW (T_g) was calculated with the first derivative of the heat flux. In the same way, the temperature at the peak (T_M), at the end of the melting endotherm of the CW–TP system (T_E), and the corresponding heat of melting (ΔH_{CW-TP}, ΔH_{TP}, or ΔH_{CW}) were calculated with the equipment software. T_g is the temperature where the first derivative of the heat capacity of the sample initially departed from the baseline. In contrast, T_M is the temperature where the first derivative of the heat capacity associated to the melting endotherm

crossed the baseline, and T_E is the temperature where it first returns to the baseline. At least two independent determinations were done at each T_{set}, and the thermal parameters were plotted as a function of the CW concentration.

Oscillatory Rheometry

Given the calorimetric results observed by the CW–TP systems investigated (i.e., the CW–1% TP solution developed organogels with T_M's that varied just between 36 °C and 38 °C, independent of the CW concentration; see "Results and Discussion"), only the organogels developed by the 3% CW–1.0% TP system at the T_{set}'s of −5 °C and 15 °C were used for rheological characterization. Previously, Morales-Rueda et al.[2] characterized the 3% CW organogels developed at 25 °C. Thus, for comparison purposes, this temperature was also included in the rheological study. The elastic (G') and loss (G'') modulus of the organogels were determined with a mechanical spectrometer (Paar Physica MCR 301, Stuttgart, Germany) using a steel cone-plate geometry (50 mm, 2°; CP50/2TG, Anton Paar, Graz, Austria) equipped with a true-gap system. This device makes the corrections in gap size associated with the expansion/shrinkage of the sample and/or the rheometer geometry due to changing temperature conditions used during measurements.[5] Temperature was controlled by a Peltier system located in both the base and top of the measurement geometry. The control of the equipment was made through the software Start Rheoplus US200/32 version 2.65 (Anton Paar, Graz, Austria). The CW–TP solution (90 °C) was applied on the base of the geometry (50 °C), and the cone was set using the true-gap function of the software. After 30 min at 90 °C, the system was cooled at 10 °C/min until achieving the corresponding T_{set}. During the cooling stage and during 60 min of the isothermal stage, G' and G″ were measured, always within the linear viscoelastic region of the CW–TP solution. At the angular frequencies used, i.e., 0.5 or 1.0 Hz, the strain (φ) applied was 0.007% or 0.02%, respectively. The modulus profile for the control systems (i.e., the 0% CW–1.0% TP and 3% CW–0% TP solutions) at each T_{set} was also determined. Two independent determinations were done and the mean of G' and G'' plotted as a function of time. G' and G'' were again measured after 120 min at T_{set}, and the corresponding organogels' yield stress (σ^*) was determined at this time by applying a strain sweep between 0% and 100%. σ^* was calculated from the log–log plot of shear stress vs. φ (percent) at the corresponding upper limit of strain. The effect of TP concentration (0% and 1%) and T_{set} (−5 °C, 15 °C, and 25 °C) on the σ^* of 3% CW organogels was established through a factorial treatment design using a completely randomized experiment design with two replicates (n=2). The results were analyzed by analysis of variance and contrast among the treatment means using STATISTICA V 7.1 (StatSoft Inc., Tulsa, OK).

Solid Phase Content

Using similar temperature conditions as for the rheological measurements, the solid phase content (SPC) of the CW–TP systems was determined by low-resolution nuclear magnetic resonance (NMR; Minispec Bruker model mq20; Bruker Analytik; Rheinstetten, Germany) after 0, 60, and 120 min of storage at each T_{set}. Then, after 30 min at 90 °C samples of the solutions (4 mL) in NMR tubes were immersed in a freezer set at −20 °C. A NMR tube with the same volume of the CW–TP solution and a thermocouple inserted was included for temperature recording. Once the systems achieved a temperature of 5 °C above the required T_{set}, the tubes were transferred into a temperature controlled bath set at −5 °C, 15 °C, or 25 °C. These conditions provided, on average, a cooling rate of 9.0 °C/min (±0.2 °C). The effect of TP concentration (0% and 1%) and T_{set} (−5 °C, 15 °C and 25 °C) on the SPC was statistically analyzed as described for σ^*. Additionally, at each T_{set} and TP concentration, the effect of storage time (0, 60, and 120 min) on SPC was evaluated using time as a repeated measurable variable (STATISTICA V 7.1; StatSoft Inc., Tulsa, OK, USA).

Texture Measurements

Force–displacement curves of the organogels were obtained with a texture analyzer (TA.XT plus; Stable Microsystems, Surrey, UK) using a flat stainless steel cylindrical probe (20 mm diameter). Thus, after 30 min at 90 °C, a given amount (≈20.0 mL) of the CW–TP solution was dispensed into transparent plastic cups (height, 3.9 cm; upper i.d., 3.5 cm; base i.d., 28 mm). The organogels obtained after 0, 60, and 120 min of storage at a given T_{set} (i.e., −5 °C, 15 °C, and 25 °C) were penetrated up to 10 mm from the surface at a speed of 1 mm/s, and then the probe was pulled out from the sample at the same speed. Using the equipment software (Texture Exponent 32; Stable Microsystems, Surrey, UK) the force displacement curves were obtained by plotting the force applied (kilogram-force) as a function of penetration depth. Analysis of the force–displacement curves provided the maximum force applied (K) and the organogel's hardness (K/mm). For a given T_{set} and storage time, at least five independent determinations were done (n=5). A temperature control chamber was used to maintain the sample temperature (i.e., T_{set}) during texture measurements. The statistical significance of the effect of TP (0% and 1%), T_{set} (−5 °C, 15 °C, and

25 °C) and time (0, 60, and 120 min) on the texture parameters of 3% CW organogels was evaluated as for σ^* and SPC.

Polarized Light Microscopy

Polarized light microphotographs (PLM) of 3% CW–1% TP organogels were obtained using a polarized light microscope (Olympus BX51; Olympus Optical Co., Ltd., Tokyo, Japan) equipped with a color video camera (KP-D50; Hitachi Digital, Tokyo, Japan) and a platina (TP94; Linkam Scientific Instruments, Ltd., Surrey England) connected to a temperature control station (LTS 350; Linkam Scientific Instruments, Ltd.) and a liquid nitrogen tank. To guarantee a uniform sample thickness, a drop of the melted sample was gently smeared over a preheated glass microscope slide (≈90 °C) using another glass slide at a 45° angle. The slide with the sample was placed on the platina, and after 30 min at 90 °C, the system was cooled (10 °C/min) to a given T_{set} (−5 °C, 15 °C, and 25 °C) with the temperature control station (Linksys32 version 1.3.1; Linkam Scientific Instruments Ltd., Waterfield, UK). PLMs of the organogels were obtained as a function of time once T_{set} was achieved. The systems with 0% CW–1% TP and 3% CW–0% TP were included in this study to evaluate the development of crystals at the corresponding T_{set}'s under conditions where no interactions occurred between the CW components and TP.

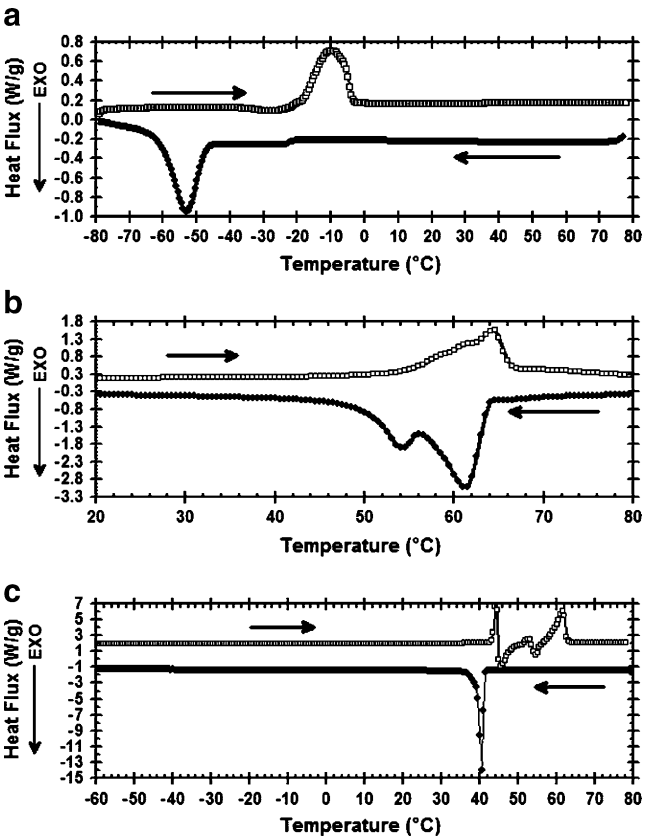

Fig. 1 Dynamic crystallization (10 °C/min) and melting (5 °C/min) thermograms for HOSFO (**a**), CW (**b**), and TP (**c**). Legends as described in the text

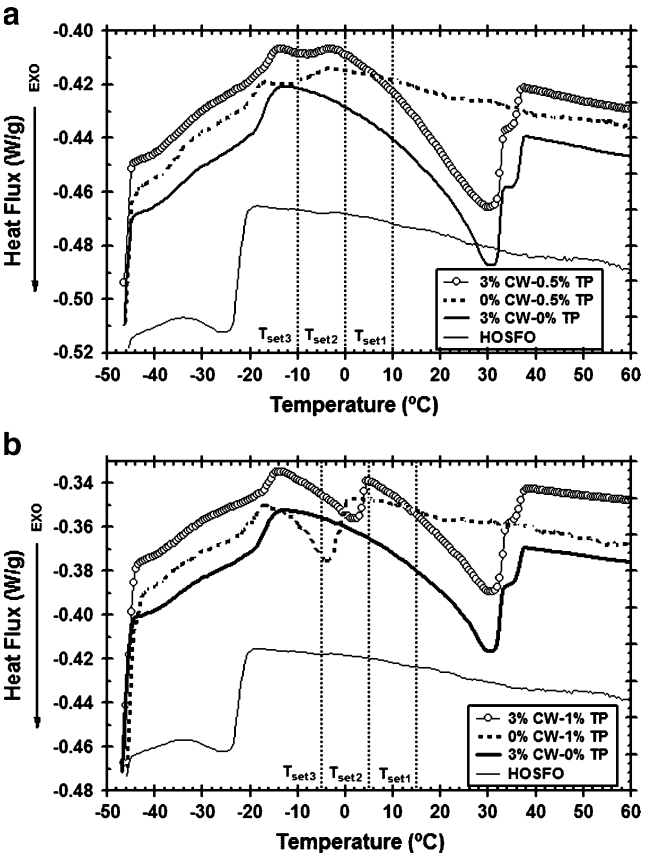

Fig. 2 Dynamic crystallization (10 °C/min) thermograms for HOSFO, CW–TP solution in HOSFO, and the corresponding control systems with 0% TP and 0% CW. The *dotted lines* indicate the T_{set}'s established to develop the 3% CW organogels with 0.5% TP and 1.0% TP

Results and Discussion

Composition and Thermal Behavior of CW, TP, and HOSFO

The specific composition of the CW and HOSFO has been reported previously.[2] The major TAGS present in HOSFO were OOO (63.32%±0.06), LnOO (17.25%±0.27), POO (8.86%±0.12), StOO (2.85%±0.07), and LnLnO (2.59%± 0.06) (P=palmitic acid, St=stearic acids, O=oleic acid, and Ln=linoleic acid). Given the high content of OOO and the high unsaturation of most TAGS present, the crystallization thermogram for HOSFO showed just one major exotherm with a crystallization onset around −20 °C and a peak crystallization temperature at ≈−53 °C. Upon heating, the HOSFO showed just one endotherm with a peak temperature at ≈−10 °C that ended at ≈−2 °C (Figure 1a).

The CW analysis showed that hentriacontane, an *n*-alkane of 31 carbons ($C_{31}H_{64}$), was its main component (78.9%±0.1%). Minor CW components included other alkanes also with odd number of carbons ($C_{29}H_{60}$, 4.2%±0.1%; $C_{33}H_{68}$, 8.0±0.2%) and triterpene alcohols with a molecular formula of $C_{30}H_{49}OH$ (i.e., germanicol, lupeol, or moretenol; 7.4%±0.1%). We have explained the cooling and heating CW thermograms previously under the base of the development of a rotator phase by the hentriacontane.[2] Rotator phases are commonly observed in *n*-alkanes and are characterized by a crystalline lattice of the molecular centers while molecules rotate about their chain axes (i.e., structural disorder).[6–8] With the exception of *n*-alkanes with even number of carbons below 22 atoms, rotator phases are present in *n*-alkanes with carbon chains from 11 to 40 atoms long.[5,6] The CW melting thermograms showed one major endotherm with a T_M of 64.42 °C (±0.23 °C), a value similar to the one reported for 99.5% pure hentriacontane (67.05 °C).[9] Based on the CW composition and the thermal parameters observed, the phase transitions of CW (Figure 1b) were mainly associated to the phase behavior of hentriacontane.

With respect to TP, the palmitic acid (93.78%±0.16%) was the major fatty acid present followed by stearic acid (3.86%±0.98%), oleic acid (0.02%±0.00), and arachidonic acid (0.02%±0.00). In consequence, the TP used showed just one major and sharp exotherm with a peak temperature at 43.18ºC (±0.23ºC) that, upon melting, showed the characteristic transitions of glyceryl tripalmitate (Figure 1c).[10–12] Thus, the first endotherm (≈44 °C) corresponded to α polymorph melting followed by the α→β′ polymorphic transition (≈45.5 °C), then melting of the β′ polymorph (≈52.5 °C) followed by the β′→β exothermic transition (≈54.5 °C), and ending with the β polymorph melting at ≈61.5 °C (Figure 1c).

Thermal Behavior of CW–TP Solutions in HOSFO

Dynamic crystallization thermograms for some CW–TP solutions in the HOSFO are shown in Figure 2. Based on the cooling thermograms of the control systems (i.e., 0% CW with 0.5% or 1% TP and 0% TP with 0.5–3% CW), the first exotherm present in the CW–TP solutions was

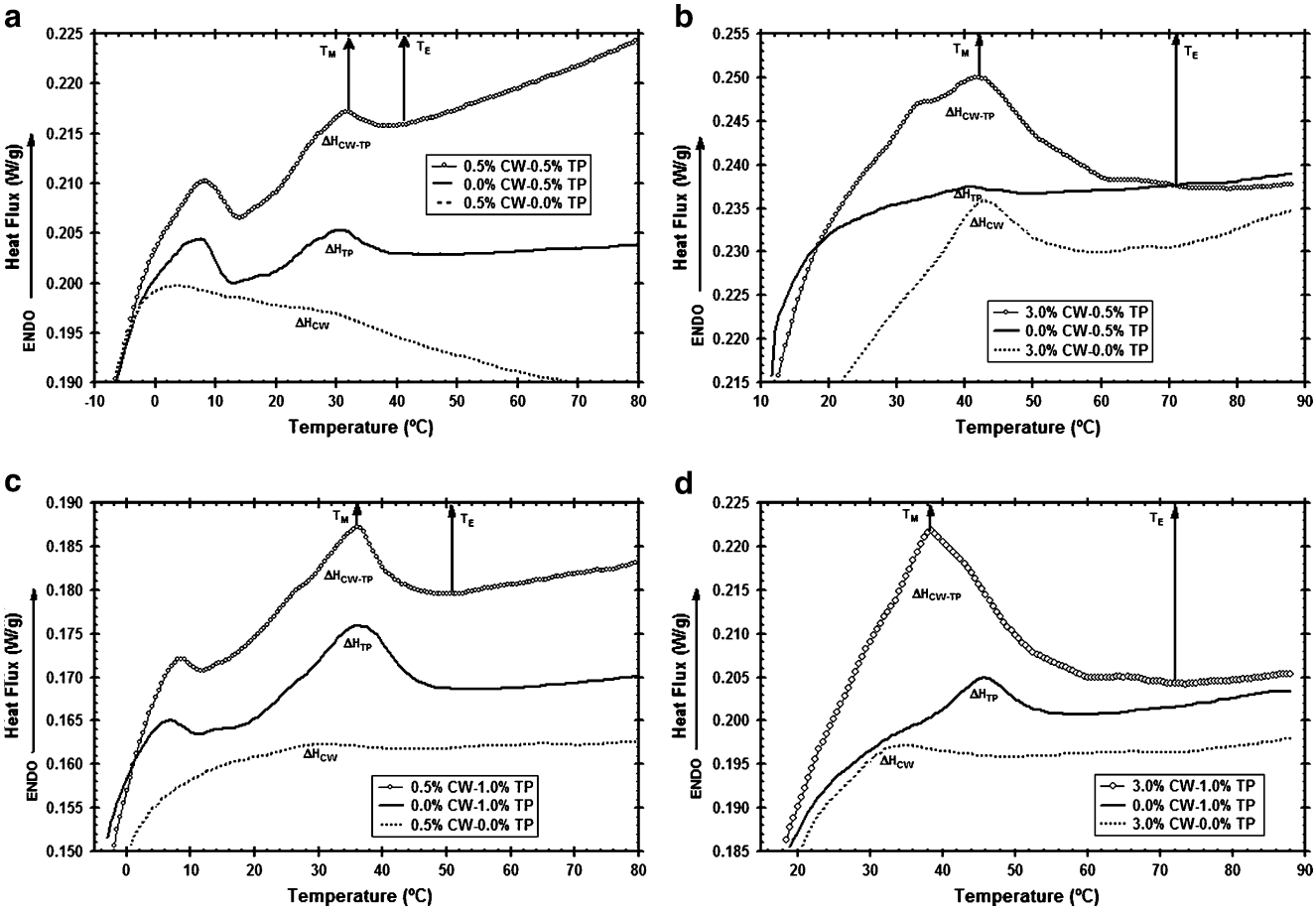

Fig. 3 Melting thermograms (5 °C/min) of organogels developed at different T_{set}'s (T_{set}=−10 °C in **a**; T_{set}=10 °C in **b**; T_{set}=−5 °C in **c**; T_{set}=15 °C in **d**) with CW–TP solutions in HOSFO and the corresponding control systems with 0% TP or 0% CW. The thermal parameters used to describe the melting behavior of the organogels are shown. Legends as described in the text

associated with CW crystallization while the second one with TP crystallization (Figure 2). With this information, the different T_{set}'s were established so that TP and CW occurred concomitantly at different supercooling extent during organogel formation. Thus, T_{set2} was the temperature at the onset of TP crystallization (i.e., beginning of the crystallization exotherm for TP) in the CW–TP blends, T_{set1} was 10 °C above T_{set2} (i.e., at approximately half way the gelation exotherm for CW in the CW–TP solutions), and T_{set3} was 10 °C below T_{set2} (i.e., at approximately half way the crystallization exotherm for TP in the CW–TP systems). In correspondence, the T_{set}'s for the CW–TP solutions with 0.5% TP were T_{set1}=10 °C, T_{set2}=0 °C, and T_{set3}=−10 °C and for the CW–TP solutions with 1.0% TP were T_{set1}= 15 °C, T_{set2}=5 °C, and T_{set3}=−5 °C (Figure 2).

In the systems where CW was present, TP crystallization occurred at a higher temperature than in the systems without CW (e.g., compare thermograms for 0% CW–1% TP and 3% CW–1% TP; Figure 2b). This phenomenon was associated with the heterogenous nucleation of TP induced by the initial crystallization of CW. These results are in line with the ones obtained by Martini et al.,[3] who observed that, under isothermal conditions, the induction time of crystallization of anhydrous milk fat decreased as the

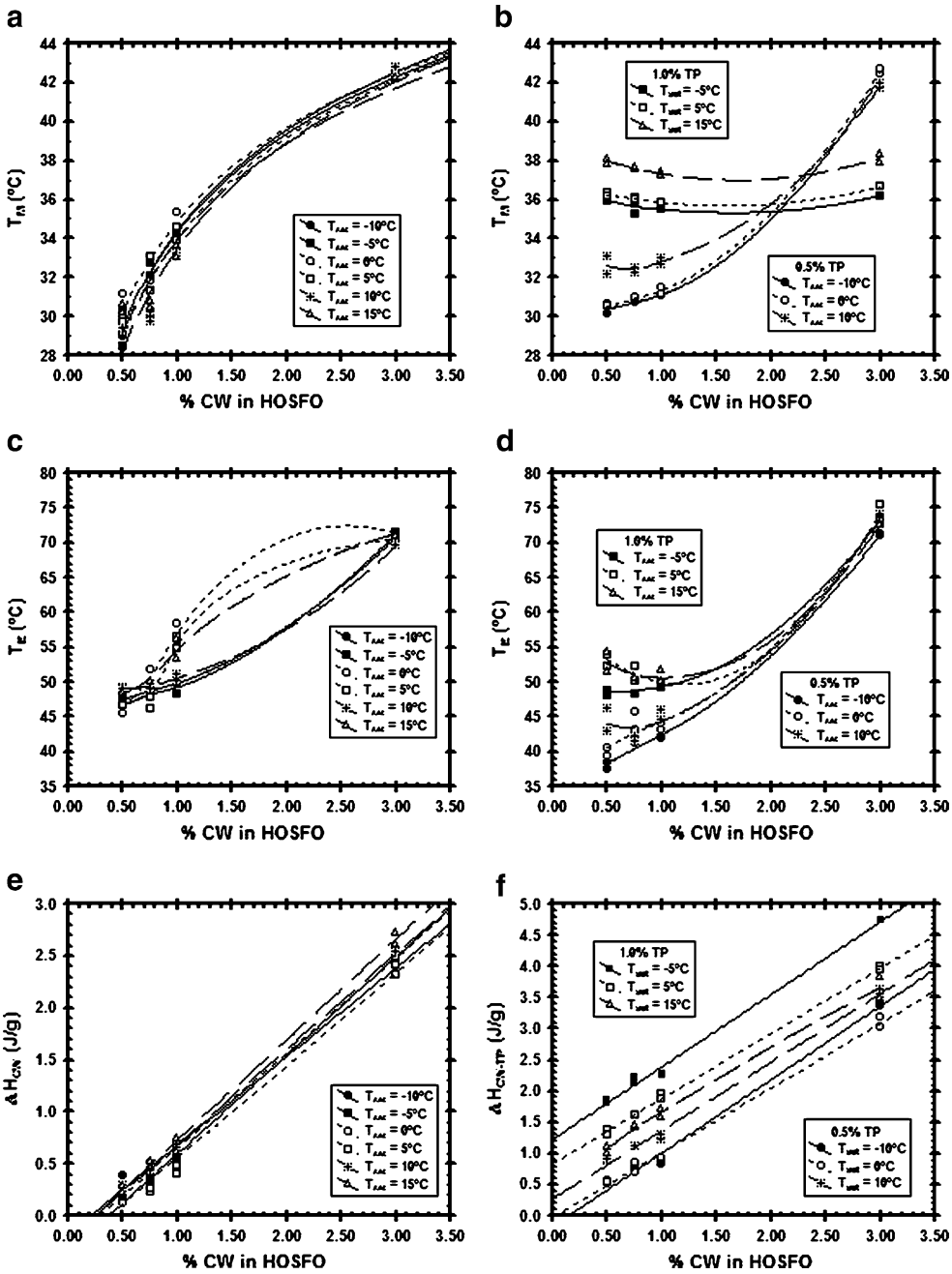

Fig. 4 Melting parameters as a function of CW concentration for organogels developed at the T_{set}'s indicated with 0% TP (**a**, **c**, and **e**), with 0.5% or with 1.0% TP (**b**, **d**, and **f**). Legends as described in the text

amount of sunflower wax increased. Given the structural similarities between the palmitic acid and the aliphatic chains of hentriacontane, the major component in CW, the crystallization process in the CW–TP solutions might result in co-crystal formation (i.e., crystals that contain two or more non-identical molecules). A minor TAGS fraction from HOSFO with an onset of crystallization at ≈−20 °C (see crystallization thermograms for HOSFO in Figure 2a, b) also seemed to co-crystallize with the CW during organogel formation (Figure 2). However, most TAGS present in the CW–TP solutions and the HOSFO crystallized below ≈−45 °C (data not shown). As a result, the organogels three-dimensional structure would be formed by co-crystals mainly constituted by CW and TP. The proportions of these components in the organogel would be determined by the composition of the CW–TP system and the supercooling conditions (i.e., the T_{set}).

The T_g of the CW–TP systems obtained at the different T_{set}'s showed similar behavior as the one observed by several *n*-alkanes when dissolved in different organic solvents,[12–14] i.e., a steady logarithmic increase as a function of CW concentration followed by a plateau (data not shown). At the CW concentrations investigated, CW observed a T_g above the T_{set}'s studied (i.e., during the non-isothermal stage). Since TP crystallized at even lower temperatures than CW, TP did not affect the T_g values nor its behavior as a function of CW concentration at any of the T_{set}'s investigated (data not shown).

Melting thermograms of organogels developed with CW–TP solutions at different T_{set}'s are shown in Figure 3. Figure 4 shows the behavior of the melting parameters for CW organogels developed with 0% TP (Figure 4a, c, e) and with 0.5% or 1.0% TP (Figure 4b, d, f) plotted as a function

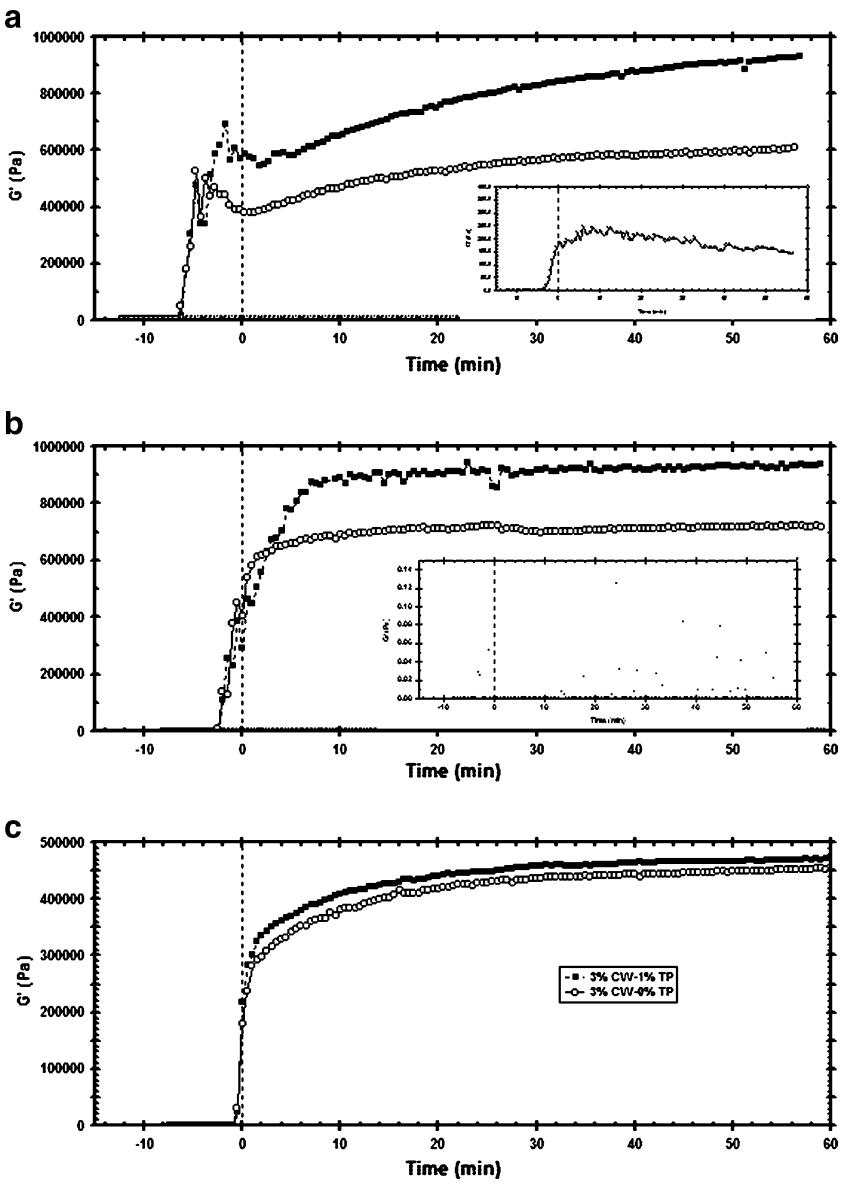

Fig. 5 *G′* profiles as a function of time for organogels developed with 3% CW-1.0% TP solution in HOSFO and the corresponding control systems, 3% CW–0% TP and 0% CW–1% TP (in the *insert*), developed at the T_{set}'s of −5 °C (**a**), 15 °C (**b**), or 25 °C (**c**). The *dotted line* indicates the beginning of the isothermal conditions

of CW concentration at each T_{set} investigated. Without TP, T_{set} seemed to affect the melting parameters of the CW organogels, particularly T_E and ΔH_{CW} (Figure 4c, e). However, this T_{set} effect was not statistically significant and was not easy to describe. In contrast, with TP the behavior of the melting parameters for the CW organogels showed a distinctive and significant effect of T_{set} and TP (Figure 4b, d, f).

Regarding the heat of melting, this parameter increased linearly as CW concentration increased (Figure 4e, f) in the systems with and without TP (Figure 4e, f). However, we observed no particular T_{set} effect in the organogels developed with 0% TP. In the organogels developed with 1% TP and at all CW concentrations investigated, the ΔH_{CW-TP} showed lower values as T_{set} increased, while in the organogels with 0.5% TP, a higher ΔH_{CW-TP} ($P<0.05$) was observed just at CW≤1.0% and at the higher T_{set} (i.e., 10 °C; Fig. 4f).

The behavior of T_M showed that, in the systems with 0% TP, this parameter increased in a curvilineal way as a function of CW concentration (Figure 4a). We observed the same behavior at all T_{set} investigated (i.e., the T_{set} effect was not statistically significant). In contrast, at 1% TP, the organogels' T_M was independent of CW concentration at all T_{set} investigated showing higher T_M values as T_{set} increased (Figure 4b), while at 0.5% TP, the T_{set} effect on T_M was evident just at CW ≤1.0% (Figure 4b). Thus, independent of CW concentration the T_M for the organogels with 1% TP was 35.81 °C (±0.36 °C) at T_{set}=−5 °C, 36.2 °C (±0.33 °C) at T_{set}=5 °C, and 37.77 °C (±0.37 °C) at T_{set}=15 °C. All these values were significantly lower than the T_M observed by the 3% CW–0.5% TP organogels but higher than the T_M of the 0.5% CW–0.5% TP, 0.75% CW–0.5% TP, and 1% CW–0.5% TP organogels developed at all T_{set}'s investigated ($P<0.05$; Figure 4b).

These results and the melting thermograms (Figure 3) showed that crystallization of TP modified the melting properties of the CW organogel. Figure 3 shows the melting thermograms for the 1% CW–0.5% TP organogel developed at T_{set} of 10 °C (Figure 3b) and the 3% CW–1% TP organogel developed at T_{set} of 15 °C (Figure 3d). Evidently, the T_M and ΔH_{CW-TP} of the CW–TP organogel showed a behavior that could not be easily associated with the corresponding parameters in the control systems (i.e., 0% CW–0.5% TP and 1% CW–0% TP for Figure 3b and 0% CW–1% TP and 3% CW–0% TP for Figure 3d). This suggested that a particular CW–TP crystal structure was developed at these supercooling conditions.

Rheology and Microstructure of the Organogels

At all T_{set}'s (i.e., −5 °C, 15 °C, and 25 °C) used in the rheology study, the onset in G' occurred before attaining isothermal conditions, and at any given T_{set}, the onset started at the same time in both the 3% CW–1.0% TP and

Table 1 Percentage of solid phase content (% SPC) and yield stress (σ^*) for organogels developed with 3% CW dispersions in HOSFO with 0% or 1% of tripalmitin (TP) at the temperatures indicated (T_{set})

T_{set} (°C)	% SPC, 0% TP		% SPC,1% TP		σ^* (Pa)		T_M (°C)		ΔH_M (J/g)	
	0min	60min[a]	0min	60min[a]	0% TP	1% TP	0% TP	1% TP	0% TP	1% TP
−5	$2.62^{A, A}$ (0.05)	$2.52^{A, A}$ (0.12)	$3.93^{A, A}$ (0.20)	$4.05^{A, A}$ (0.009)	$378.15^{A, A}$ (2.25)	$682.04^{A, B}$ (292.54)	$42.64^{A, A}$ (0.03)	$36.21^{A, B}$ (0.00)	$2.50^{A, A}$ (0.01)	$4.73^{A, B}$ (0.00)
15	$2.40^{B, A}$ (0.11)	$2.43^{A, A}$ (0.14)	$2.59^{B, A}$ (0.12)	$3.39^{B, B}$ (0.08)	$402.97^{A, A}$ (66.38)	$932.34^{A, B}$ (462.70)	$42.25^{A, A}$ (0.01)	$38.16^{B, B}$ (0.28)	$2.67^{B, A}$ (0.07)	$3.66^{B, B}$ (0.24)
25	$2.22^{C, A}$ (0.04)	$2.10^{B, A}$ (0.08)	$2.09^{C, A}$ (0.09)	$2.39^{C, B}$ (0.07)	$228.06^{A, A}$ (24.94)	$230.98^{B, A}$ (54.72)	$42.14^{A, A}$ (0.01)	$42.28^{C, A}$ (0.30)	$3.78^{C, A}$ (0.48)	$4.02^{C, A}$ (0.41)

For the same column, the same uppercase superscripted first letter indicates that the values are statistically equal. A different uppercase superscripted letter indicates that the values for the same column are significantly different ($P<0.05$) (i.e., the T_{set} effect was significant). For the same row and parameter, the same uppercase superscripted second letter indicates that the values are statistically equal. A different uppercase superscripted letter indicates that the values for the same row and parameter are significantly different ($P<0.05$) (i.e., the time effect or the TP effect was significant). The time at which the% SFC was measured is indicated. The values are reported as the mean and standard deviation of at least two independent determinations

[a] The % SPC values after 60 and 120 min were statistically the same in all cases but for the 3% CW–0% TP at T_{set}=−5 °C. When the % SPC values were equal statistically the same, the values were averaged and the mean and standard deviation reported

the 3% CW-0% TP systems. As previously indicated, CW crystallization (i.e., $T_g \approx 38$ °C) occurred before attaining the corresponding T_{set} (Figure 2). Therefore, the G' onset of both the 3% CW–1.0% TP and the 3% CW–0% TP systems was associated with CW crystallization. The G' onset of the 0% CW–1.0% TP control system at the T_{set} of −5 °C (see the insert of Figure 5a) also occurred before attaining isothermal conditions. DSC analysis showed that, in this control system, TP crystallization occurred during the cooling stage at ≈3.5 °C. At the T_{set}'s of 15 °C (insert of Figure 5b) and 25 °C, a limited or no increase in G' was observed in this control system, and DSC analysis confirmed that no TP crystallization occurred during the cooling stage.

Once isothermal conditions were attained at all T_{set}'s, G' increased logarithmically in both the 3% CW–1.0% TP and the 3% CW–0% TP systems until a plateau was achieved (Figure 5), this particularly at the T_{set} of 15 °C (Figure 5b) and 25 °C (Figure 5c). Overall, the increase in the elasticity as a function of time monitored the development of the three-dimensional structure that resulted in the CW–TP organogel formation. Within this framework, it is important to point out that, at all T_{set} investigated, the 3% CW–1.0% TP organogels achieved higher G' values than the 3% CW–0% TP organogels, and this difference increased as T_{set} decreased (Figure 5). This was explained considering that, at all T_{set} investigated, higher SPC was obtained in the CW organogels with 1% TP than in the organogels without TP ($P<0.05$; Table 1). However, for a given T_{set}, the co-crystallization of TP with CW seemed to modify the three-dimensional organization of the CW organogel in a limited way. This is because, for a given T_{set}, the 3% CW organogels developed with and without TP, showed similar G' behavior during organogel formation (Figure 5).

On the other hand, the increase in G' during the isothermal stage (Figure 5a–c) could not be fully explained by the changes in SPC during organogel development (Table 1). This is because, in the system with 0% TP and at all T_{set}'s studied, the SPC achieved once isothermal conditions were attained (i.e., time=0 min) remained constant even after 120 min in all cases but for T_{set}=−5 °C. (Table 1). At this particular T_{set}, the SPC after 120 min was 2.74% (±0.08%), a value significantly higher ($P<0.05$) than the one at 60 min [2.52% (±0.12%); Table 1]. In contrast, in the 3% CW-1.0% TP organogels, the SPC achieved at time= 0 min remained constant during 120 min just at T_{set}=−5 °C (i.e., at the highest supercooling, TP crystallized during the cooling stage, and no additional TP crystallization occurred

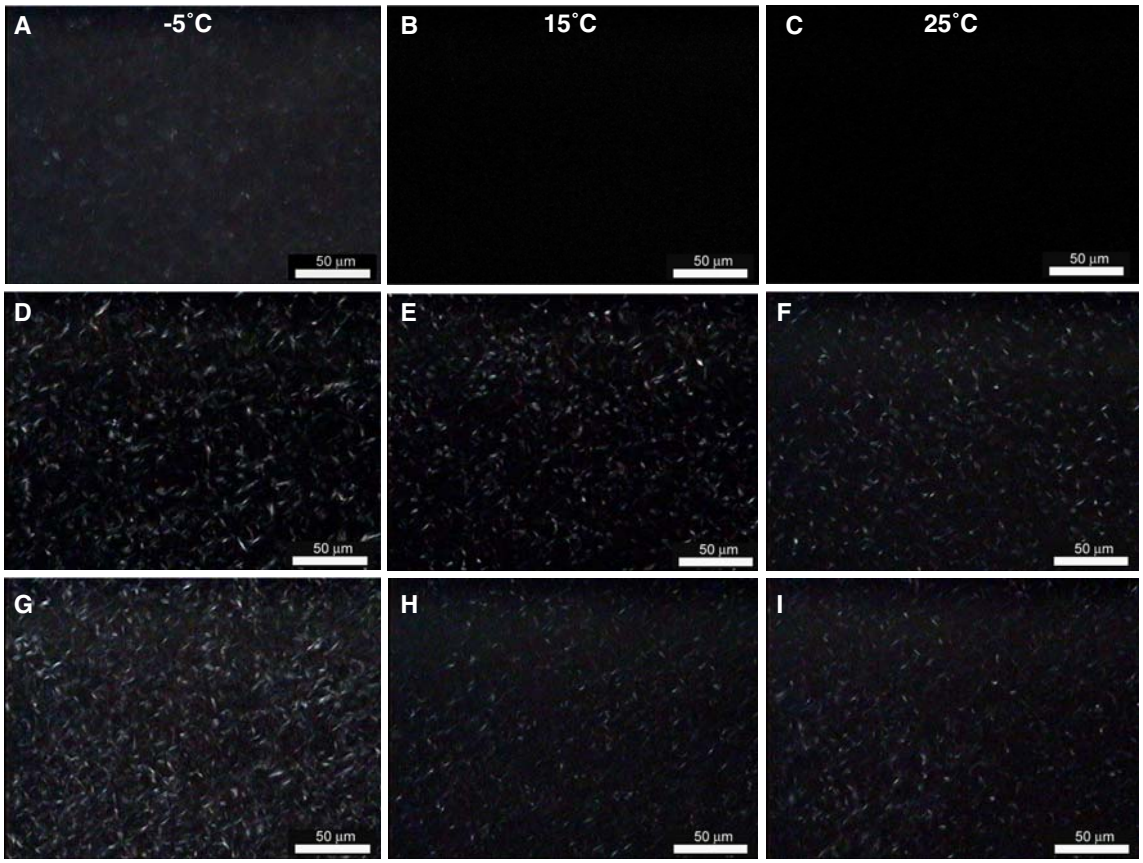

Fig. 6 Microphotographs of the 0% CW–1% TP (**a**–**c**), 3% CW–0% TP (**d**–**f**), and the 3% CW–1% TP (**g**–**i**) organogels after achieving isothermal conditions (0 min) at the T_{set}'s indicated. For the *same column*, the same T_{set} applies

during the isothermal stage). At the T_{set}'s of 15 °C and 25 °C, the SPC of the 3% CW–1.0% TP organogels continued increasing during the isothermal stage, achieving a constant value after 60 min ($P<0.05$) (i.e., TP crystallized during the cooling stage and the first 60 min of the isothermal stage).

A particular rheological behavior was observed at the T_{set} of 15 °C in both the 3% CW–1.0% TP and the 3% CW–0% TP systems. Under isothermal conditions, these two systems showed a higher rate of G' increase and G' achieved a plateau at a higher value at $T_{set}=15$ °C (Figure 5b) than at $T_{set}=-5$ °C (Figure 5a). This was regardless of the lower SPC present at $T_{set}=15$ °C in comparison with the SPC at $T_{set}=-5$ °C ($P<0.05$; Table 1). As already pointed out, the melting thermograms of the 3% CW–1.0% TP organogel developed at 15 °C (Figure 3d) suggested that, at this supercooling conditions, a particular CW–TP crystal structure was developed. This structure might be associated with the evolution of the hentriacontane's (i.e., the major gelator compound in CW) rotator phase into a higher order structural state and its impact on the mechanical properties of the organogel's three-dimensional network. This explanation was already suggested by Morales-Rueda et al.,[2] obtained through rheological and DSC measurements of CW organogels developed at 5 °C and 25 °C. A similar explanation might apply to the G' behavior observed at $T_{set}=25$ °C (Figure 5b). However, at this temperature, a lower SPC was obtained than at T_{set}'s of −5 °C and 15 °C (Table 1), and therefore, the G' profile was lower than at T_{set}'s of −5 °C and 15 °C (Figure 5). The increase in ΔH_M, particularly observed in the 3% CW–0% TP system as T_{set} increased (Table 1) and approached the melting temperature of CW in the organogel, is in agreement with the occurrence of an annealing process (i.e., perfection of the crystalline regions and/or ordering of amorphous regions). In biopolymers such as starch, annealing, as measured by the increase in ΔH_M and X-ray diffraction, is more effective at temperatures just below the melting temperature.[15,16]

At this level, it is important to point out that the CW organogels developed at 25 °C by Morales-Rueda et al.,[2] showed a steady and significant G' decrease as a function of time until attaining a plateau at approximately 140 min.[2] In the present research, the organogels did not observe such G' decrease, despite the fact that the same batch of CW was used in both investigations. However, the rheometer used by Morales-Rueda et al.[2] (Paar Physica UDS 200; Stuttgart, Germany) was not equipped with a real-gap system as was the rheometer used in the present investigation. For the

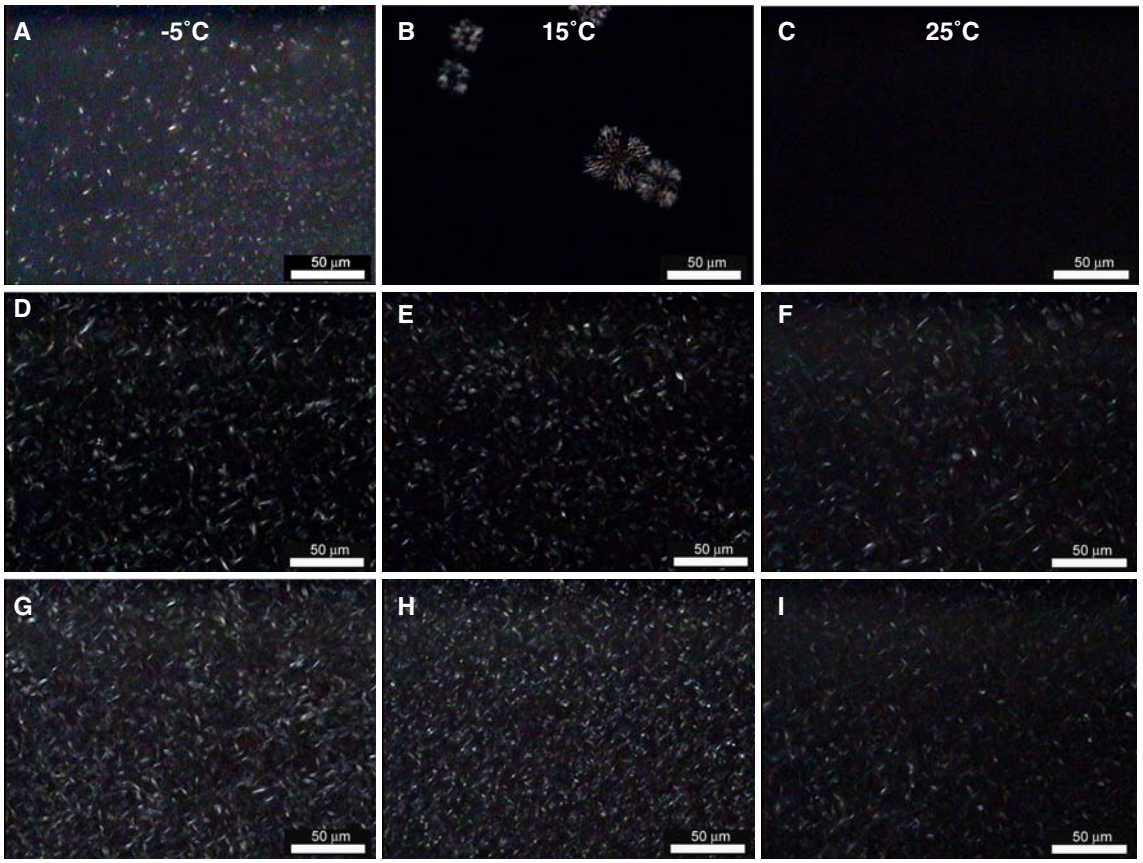

Fig. 7 Microphotographs of the 0% CW–1% TP (**a**–**c**), 3% CW–0% TP (**d**–**f**), and the 3% CW–1% TP (**g**–**i**) organogels after 60 min at the T_{set}'s indicated. For the *same column* the same T_{set} applies

rheological measurements, those authors[2] used a constant gap of 0.05 mm provided by a cone (50 mm, 17) and plate geometry (MK-22). Then, the expansion/shrinkage suffered by the CW organogel during its development at any T_{set} affected G' measurements. In consequence, the G' profile observed by Morales-Rueda et al.[2] for CW organogels might be affected by the lack of correction in gap size and the subsequent normal force effect on G′ measurements.[5]

Microphotographs of the controls (i.e., 0% CW–1% TP and 3% CW–0% TP) and the 3% CW–1% TP systems at 0, 60, and 120 min at the T_{set} investigated are shown in Figures 6, 7, and 8, respectively. In particular, the microphotographs for the 0% CW–1% TP system showed that TP did not crystallize at the T_{set} of 25 °C even after 120 min (Figures 6c, 7c and 8c). However, at the T_{set} of −5 °C, the TP crystallized during the cooling stage as small crystals (Figure 6a), and at 15 °C, spherulite-shaped crystals appeared after ≈7.5 min of achieving isothermal conditions (data not shown). These spherulites became larger as a function of time (Figures 7b and 8b). The TP crystals developed at a T_{set} of −5 °C had a T_M of 35.6 °C (±0.7 °C) and a ΔH_M of 1.70 J/g (±0.06 J/g), while the ones developed at a T_{set} of 15 °C had a T_M of 45.9 °C (±0.4 °C) and a ΔH_M of 0.89 J/g (0.12 J/g). Although no X-ray analysis was done, these results showed that TP crystallized in the HOSFO in different polymorph states, probably as α at the T_{set} of −5 °C and as β′ at the T_{set} of 15 °C.

The microphotographs of the 3% CW–0% TP system showed the characteristic microcrystalline structure developed by CW organogels (Figure 6d–f).[1,2] These microphotographs showed that, for a given T_{set}, the numbers of crystals that form the CW organogel three-dimensional structure seemed to remain constant as a function of time. This observation applied for all T_{set}'s investigated (i.e., Figure 6d, 7d, and 8d).

The microphotographs corresponding to the 3% CW–1% TP organogels (Figures 6g–i, 7g–i, and 8g–i) showed the presence of higher number of crystals than the 3% CW–0% TP organogels (Figures 6d–f, 7d–f, and 8d–f), particularly at the T_{set}'s of −5 °C and 15 °C. At the T_{set}=−5 °C, the number of crystals in the 3% CW–1% TP organogels apparently remained constant as a function of time (i.e., Figures 6g, 7g, and 8g). However, at higher T_{set}'s the number of crystals increased from time=0 min to time= 60 min (i.e., Figures 6i and 7i), and this increase was more evident at the T_{set} of 15 °C (Figures 6h and 7h). Additionally, at this T_{set}, distinctive small and highly birefringent crystals, probably resulting from TP crystalli-

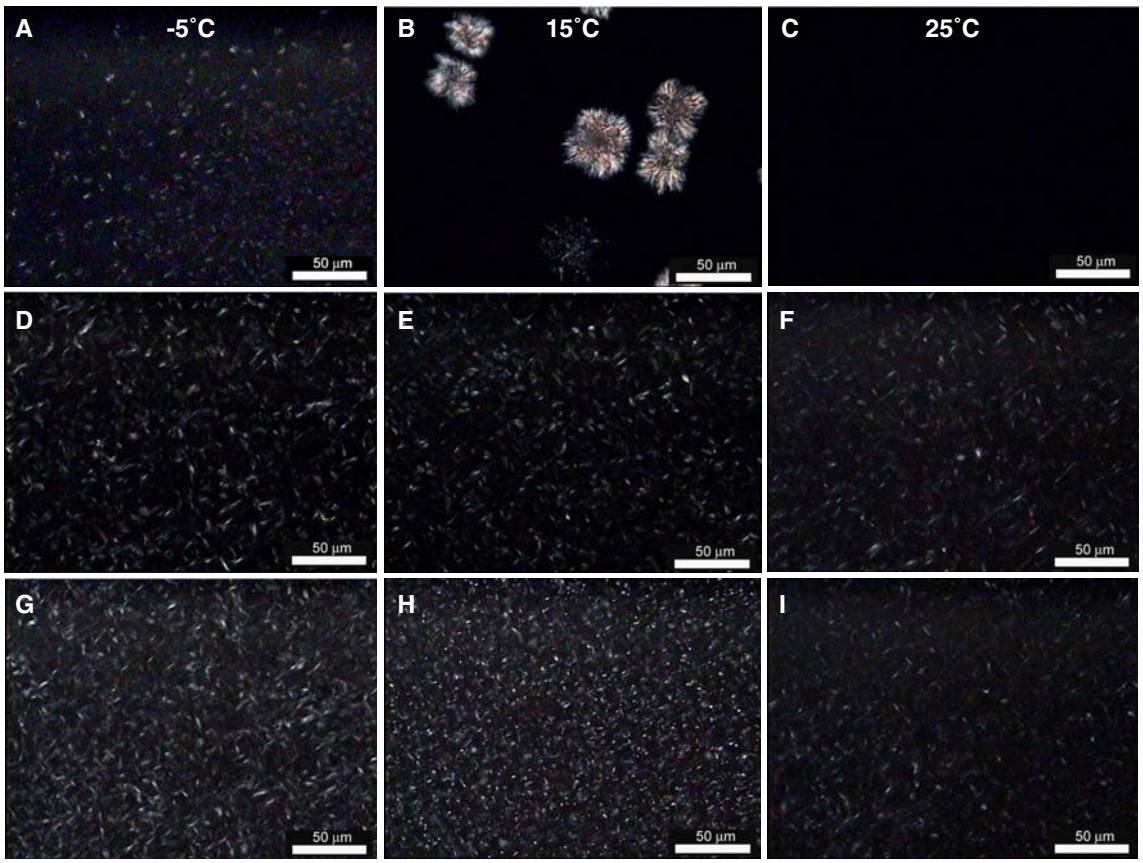

Fig. 8 Microphotographs of the 0% CW–1% TP (**a**–**c**), 3% CW–0% TP (**d**–**f**), and the 3% CW–1% TP (**g**–**i**) organogels after 120 min at the T_{set}'s indicated. For the *same column* the same T_{set} applies

zation, appeared around 60 min (Figure 7h). Apparently, after 60 min, the number of crystals remained constant at all T_{set}'s studied. These results agreed with the SPC behavior (Table 1) and with the higher G' profile observed by the 3% CW–1% TP organogels in comparison with the one showed by the 3% CW–0% TP organogels (Figure 5). The particular crystallization behavior occurring at the T_{set} of 15 °C, resulted, as already mentioned, in organogels with particular G' profiles also evident in the yield stress (σ*) behavior. Thus, in CW, organogels developed without TP, the T_{set} did not affect σ* (Table 1). In contrast, with the 3% CW–1.0% TP organogels, there was a tendency to obtain higher σ* at the T_{set} of 15 °C than at the T_{set}'s of −5 °C and 25 °C. Nevertheless, the σ* of the organogels developed at the T_{set}'s of −5 °C and 15 °C were statistically the same, and both σ* values were higher than the one obtained at T_{set} of 25 °C ($P<0.10$; Table 1). Then, the 3% CW–1.0% TP organogels developed at a T_{set} of 15 °C had higher elasticity but similar resistance to permanent (i.e., plastic) deformation than the organogels developed at the T_{set} of −5 °C. This is regardless of the lower SPC obtained at the T_{set} of 15 °C

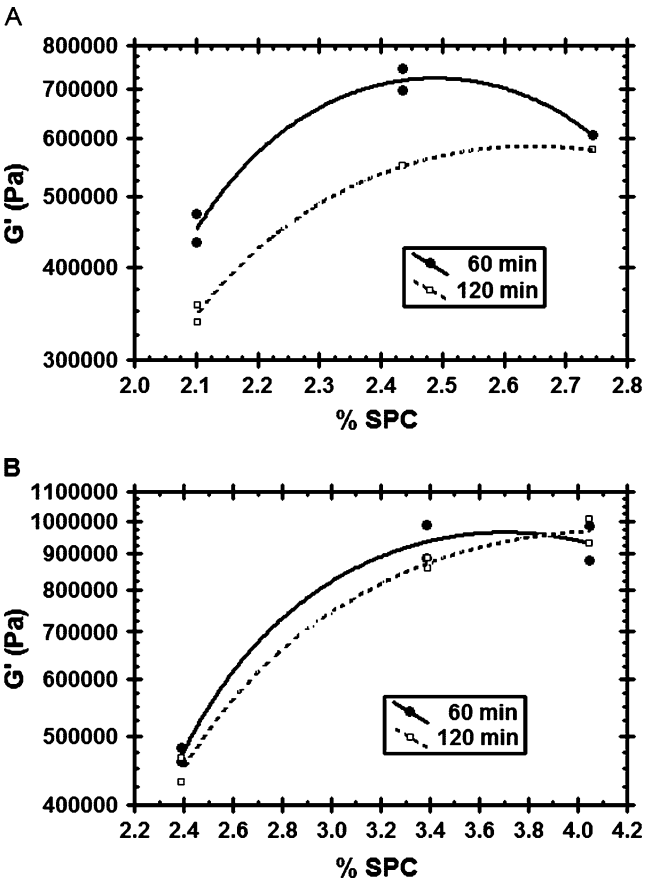

Fig. 9 G' after 60 min and 120 min at the corresponding T_{set} for the 3% CW–0% TP (**a**) and 3% CW–1% TP (**b**) organogels as a function of SPC. Legends as described in the text

Table 2 Textural parameters of the 3% CW organogels obtained with (1% TP) and without (0%) TP at different T_{set}

Time at T_{set} (min)	T_{set}=−5°C				T_{set}=15°C				T_{set}=25°C			
	Maximum force (K)		Hardness (K/mm)		Maximum force (K)		Hardness (K/mm)		Maximum force (K)		Hardness (K/mm)	
	0% TP	1% TP	0% TP	1% TP	0% TP	1% TP	0% TP	1% TP	0% TP	1% TP	0% TP	1% TP
0	$0.388^{A,A}$ (0.056)	$0.585^{A,B}$ (0.038)	$2.425^{A,A}$ (0.179)	$3.105^{A,B}$ (0.239)	$0.361^{A,A}$ (0.066)	$0.302^{A,A}$ (0.013)	$2.252^{A,A}$ (0.489)	$2.055^{A,A}$ (0.054)	$0.186^{A,A}$ (0.036)	$0.212^{A,A}$ (0.038)	$1.497^{A,A}$ (0.352)	$1.421^{A,A}$ (0.115)
60	$0.440^{A,A}$ (0.021)	$0.597^{A,B}$ (0.064)	$2.389^{A,A}$ (0.236)	$3.446^{A,B}$ (0.271)	$0.343^{A,A}$ (0.055)	$0.298^{A,A}$ (0.008)	$2.262^{A,A}$ (0.519)	$2.122^{A,A}$ (0.098)	$0.182^{A,A}$ (0.015)	$0.215^{A,A}$ (0.051)	$1.497^{A,A}$ (0.323)	$1.368^{A,A}$ (0.089)
120	$0.446^{A,A}$ (0.019)	$0.612^{A,B}$ (0.031)	$2.509^{A,A}$ (0.161)	$3.611^{A,B}$ (0.433)	$0.329^{A,A}$ (0.039)	$0.323^{A,A}$ (0.020)	$2.292^{A,A}$ (0.374)	$2.213^{A,A}$ (0.077)	$0.169^{A,A}$ (0.010)	$0.211^{A,A}$ (0.061)	$1.523^{A,A}$ (0.364)	$1.443^{A,A}$ (0.090)

For the same column, the same uppercase superscripted first letter indicates that the values are statistically equal. A different uppercase superscripted letter indicates that the values for the same column are significantly different ($P<0.05$) (i.e., the time effect was significant). For the same row and parameter, the same uppercase superscripted second letter indicates that the values are statistically equal. A different uppercase superscripted letter indicates that the values for the same row and parameter are significantly different ($P<0.05$) (i.e., the TP effect was significant)

in comparison with the SPC present at the T_{set} of −5 °C (Table 1).

When the G' at 60 and 120 min of the 3% CW–0% TP and the 3% CW–1% TP organogels were plotted as a function of SPC, in both cases, the elasticity of the organogels increased steadily as a function of SPC (Figure 9). However, after 60 min, the G' of the 3% CW organogels developed without TP decreased ($P<0.05$), and this decrease was larger as SPC decreased (i.e., as T_{set} increased; Figure 9a). Such behavior was not observed in the 3% CW–1% TP organogels at any of the SPC (i.e., T_{set}) present in the organogels (Figure 9b). Co-crystallization of TP with the CW also resulted in organogels with lower T_M and higher ΔH_M than the ones shown by the 3% CW–0% TP organogels (Table 1), and this difference increased as T_{set} decreased (Table 1). From here, it is evident that the interaction between TP and CW during crystallization resulted in organogels with different thermomechanical properties than CW organogels.

Texture of the Organogels

Except for the organogels developed at T_{set}=−5 °C, the maximum force applied and the relative hardness were statistically the same in both the 3% CW–0% TP and the 3% CW–1% TP organogels, and we observed this behavior at 0, 60, and 120 min (Table 2). It is important to point out that the maximum force in the 3% CW–0% TP organogels developed at the T_{set}'s of 15 °C and 25 °C decreased as a function of time. However, the time effect on this textural parameter was not significant (Table 2). In contrast, in the 3% CW–1% TP organogels at the same T_{set}'s, both the maximum force and the hardness did not show this behavior. At T_{set}=−5 °C, the 3% CW–1% TP organogels showed higher textural values than the 3% CW–0% TP organogels at all times investigated ($P<0.05$; Table 2). At this T_{set}, the difference in hardness between the CW organogels developed with and without TP increased the longer the storage time (i.e., the 3% CW–1% TP organogels became harder than the 3% CW–0% TP organogels as time increased; Table 2). Then, the behavior of the textural parameters in both types of organogels was in correspondence with the G' results shown in Figure 9.

From the above, co-crystallization of TP with CW evidently had an effect on both the mechanical and thermal properties of the organogel. At this level and without X-ray analysis, no particular model is proposed for the possible crystal structure developed by TP and CW. However, given the structural similarities between the aliphatic chains of hentriacontane and the ones of palmitic acid in the TP, envisioning the development of mixed lamellar structures is easy. Ongoing X-ray studies are trying to elucidate the TP–CW crystal structure at the different T_{set}'s investigated. On the other hand, the results obtained by rheology under low deformation showed that, at T_{set}=15 °C, the TP–CW crystal developed an organogel with a reinforced three-dimensional network. This is in comparison with the structure developed by the CW organogel. However, such structural reinforcement might not be strong enough when a force beyond σ^* was applied (i.e., texture measurements), and therefore, the organogels suffered permanent deformation in the same way as the CW organogels. This, regardless the higher SPC present in the 3% CW–1% TP organogels than in the 3% CW–0% TP organogels (Table 1). Under such conditions, higher textural parameters might be obtained with the 3% CW–1% TP organogels just at the lowest supercooling conditions investigated (T_{set}=−5 °C), this is comparison with the 3% CW–0% TP organogels.

Conclusions

The interaction of TP and CW during organogel formation resulted in a three-dimensional crystal network with thermomechanical properties different from the one obtained just by CW organogels. The results and the ones obtained by Martini et al.[3] showed that the triacylglycerides–wax (i.e., sunflower oil wax, CW, and carnauba wax) interaction during crystallization might be a useful alternative to tailor particular physicochemical properties associated to a specific functionality (i.e., melting profile and texture). Organogelation of vegetable oil might be used to develop *trans*-free vegetable-oil-based spreads and coatings and also novel food products with distinctive textural perceptions for the consumers.

Acknowledgments The investigation was supported by grant no. 48273-Z/25706 from CONACYT. The technical support from Concepcion Maza-Moheno and Elizabeth Garcia-Leos is greatly appreciated.

References

1. J.F. Toro-Vazquez, J.A. Morales-Rueda, E. Dibildox-Alvarado, M.A. Charó-Alonso, M. Alonzo-Macías, M.M. González-Chávez, Development of organogels with candelilla wax and safflower oil with high triolein content. J Am Oil Chem Soc **84**, 989–1000 (2007). doi:10.1007/s11746-007-1139-0
2. J.A. Morales-Rueda, E. Dibildox-Alvarado, M. Charó-Alonso, R.G. Weiss, J.F. Toro-Vazquez, Thermo-mechanical properties of candelilla wax and dotriacontane organogels in safflower oil. Eur J Lipid Sci Technol **111**, 207–215 (2009). doi:10.1002/ejlt.200810174
3. S. Martini, A.A. Carelli, J. Lee, Effect of the addition of waxes on the crystallization behavior of anhydrous milk fat. J Am Oil Chem Soc **85**, 1097–1104 (2008). doi:10.1007/s11746-008-1310-2
4. J.F. Toro-Vazquez, E. Dibildox-Alvarado, M.A. Charó-Alonso, V. Herrera-Coronado, C.A. Gómez-Aldapa, The Avrami index and the fractal dimension in vegetable oil crystallization. J Am Oil Chem Soc **79**, 855–866 (2002). doi:10.1007/s11746-002-0570-y
5. J. Läuger, A. Ziegler, G. Raffer, True gap control: direct measurement of the real gap size during parallel-plate and cone and plate rheological experiments. Rev Mex Ing Quim **3**, 307–310 (2004)

6. P. Espeau, J.W. White, Thermodynamic properties of *n*-alkanes in porous graphite. J Chem Soc Faraday Trans **93**, 3197–3200 (1997). doi:10.1039/a701074e
7. B. Zgardzinska, M. Pietrow, T. Goworek, J. Wawryszczuk, *Ortho*-positronium in some *n*-alkanes; influence of temperature and pressure. Acta Phys Pol A **110**, 747–753 (2006)
8. K. Tozaki, H. Inaba, H. Hayashi, C. Quan, N. Nemoto, T. Kimura, Phase transitions of n-$C_{32}H_{66}$ measured by means of high resolution and super-sensitive DSC. Therm Acta **397**, 155–161 (2003). doi:10.1016/S0040-6031(02)00273-3
9. INFOTHERM (2006) http://www.fiz-chemie.de/infotherm/servlet/infothermSerch.
10. S. Kiyotaka, T. Kuroda, Kinetics of melting crystallization and transformation of tripalmitin polymorphs. J Am Oil Chem Soc **64**, 124–127 (1987). doi:10.1007/BF02546266
11. T. Sonoda, Y. Takata, S. Ueno, K. Sato, DSC and synchrotron-radiation X-ray diffraction studies on crystallization and polymorphic behavior of palm stearin in bulk and oil-in-water emulsion states. J Am Oil Chem Soc **81**, 365–373 (2004). doi:10.1007/s11746-004-0908-5
12. J.F. Toro-Vazquez, E. Dibildox-Alvarado, M.A. Charó-Alonso, Determination of some crystallization parameters for triacylglycerides of vegetable oils. Food Sci Technol Int **5**, 67–78 (1999). doi:10.1177/108201329900500107
13. D.J. Abdallah, L. Lu, R.G. Weiss, Thermoreversible organogels from alkane gelators with one heteroatom. Chem Mater **11**, 2907–2911 (1999). doi:10.1021/cm9902826
14. D.J. Abdallah, R.G. Weiss, *n*-Alkanes gel *n*-alkanes (an many other organic liquids). Langmuir **16**, 352–355 (2000). doi:10.1021/la990795r
15. R. Hoover, T. Vasanthan, The effect of annealing on the physicochemical properties of wheat, oat, potato and lentil starches. J Food Biochem **17**, 303–325 (1994). doi:10.1111/j.1745-4514.1993.tb00476.x
16. K. Köhler, G. Förster, A. Hauser, B. Dobner, U.F. Heiser, F. Ziethe, W. Richter, F. Steiniger, M. Drechsler, H. Stettin, A. Blume, Temperature-dependent behavior of a symmetric long-chain bolaamphiphile with phosphocholine headgroups in water: from hydrogel to nanoparticles. J Am Chem Soc **126**, 16804–16813 (2004). doi:10.1021/ja046537k